Desalination and Water Treatment
www.deswater.com

doi: 10.1080/19443994.2015.1029010

57 (2016) 7881–7897
April

Taylor & Francis
Taylor & Francis Group

Optimization of microwave irradiated - coconut shell activated carbon using response surface methodology for adsorption of benzene and toluene

Jibril Mohammed[a,b,c], Noor S. Nasri[d,*], Muhammad A. A. Zaini[b,e], Usman D. Hamza[a,b,c], Husna M. Zain[a], Farid Nasir Ani[f]

[a]*UTM-MPRC Institute for Oil and Gas, Energy Research Alliance, Research University, Universiti Teknologi Malaysia, 81310 UTM Johor Bahru, Johor, Malaysia, Tel. +60 167657458; email: jibrilmuhammad@gmail.com (J. Mohammed), Tel. +60 192651147; email: udhamza2@gmail.com (U.D. Hamza), Tel. +60 148086599; email: husnamdzain@gmail.com (H.M. Zain)*
[b]*Faculty of Chemical Engineering, Chemical Engineering Department, Research University, Universiti Teknologi Malaysia, 81310 UTM Johor Bahru, Johor, Malaysia, Tel. +60 162581878; email: abbas@cheme.utm.my (M.A.A. Zaini)*
[c]*Chemical Engineering Department, Abubakar Tafawa Balewa University, P.M.B 0248 Bauchi, Nigeria*
[d]*Sustainability Waste-to-Wealth Unit, UTM-MPRC Oil and Gas Institute, Energy Research Alliance, Universiti Teknologi Malaysia, 81310 UTM Johor Bahru, Johor, Malaysia, Tel. +60 137728200; email: noorshaw@petroleum.utm.my*
[e]*Centre of Lipids Engineering & Applied Research (CLEAR), Ibnu Sina ISIR, Universiti Teknologi Malaysia, 81310 UTM Johor Bahru, Johor, Malaysia*
[f]*Faculty of Mechanical Engineering, Universiti Teknologi Malaysia, 81310 Skudai, Johor, Malaysia, Tel. +60 137474714; email: farid@mail.fkm.utm.my*

Received 25 December 2014; Accepted 7 March 2015

ABSTRACT

Effluents from various industries release volatile organic compounds (VOCs) into the environment which causes serious environmental hazards. Coconut shell-based porous carbons were synthesized using chemical activation with potassium hydroxide (KOH) for adsorption of benzene and toluene. Central composite design of the response surface methodology was used in the optimization of the preparation conditions of the porous carbons. The effects of microwave power, irradiation time, and KOH impregnation ratio (IR) on benzene and toluene removal were investigated. The optimum condition was obtained at microwave power of 500 W; irradiation time 4 min; and 1.5 KOH IR, which resulted in 84 and 85% removal of benzene and toluene, respectively, at 95% yield of activated carbon (AC) from the char. Equilibrium data were fitted to Langmuir, Freundlich, and Temkin isotherms with all the models having $R^2 > 0.94$. The equilibrium data were best fitted by Langmuir isotherm, with maximum adsorption capacity of 212 and 238 mg/g for benzene and toluene, respectively. High surface area of 1,354 m^2/g and highly microporous carbon prepared lead to the high adsorption capacities. Pseudo-second-order kinetic model best fitted the kinetic data. The ACs produced can be used to remediate water polluted by VOCs.

*Corresponding author.

Presented at the 7th International Conference on Challenges in Environmental Science and Engineering (CESE 2014) 12–16 October 2014, Johor Bahru, Malaysia

Keywords: Adsorption; Water treatment; Environmental hazard; Microwave chemical activation; Volatile organic compounds; Response surface methodology

1. Introduction

Considerable concerns have been raised all over the world over the presence of volatile organic compounds (VOCs) in the environment, because gaseous effluents and produced water from process industries like refineries, pharmaceuticals, paint, gasoline from filling stations, solvents for manufacturing industries, transportation, and auto exhausts release VOCs into the atmosphere and aqueous environment which causes serious environmental challenges. Studies have also reported that the presence of different VOCs in drinking water in 11 states at peninsular Malaysia was attributed to the improper disposal practice [1,2]. Many of these VOCs are hazardous to human health and the environment as they are flammable, toxic, carcinogenic, and mutagenic agents [3–10]. Many are also compounds of fuels, solvents, hydraulic fluids, and dry cleaning agents commonly used in urban settings such as bleach [11]. Air stripping, absorption, reverse osmosis, biological, thermal and catalytic oxidation, sonochemical, and other advanced oxidation processes like Fenton, photo-Fenton, wet oxidation, ozonation, photo catalysis, electrochemical, membrane-based separation, and non-thermal plasma are among the treatment methods used to remediate VOCs in water [11], but they all have certain limitations in terms of efficiency and cost.

Adsorption of various contaminants by activated carbon (AC) has proven to be sustainable, environmentally friendly, economical, and efficient which makes it the most commonly used technique [9,12–14]. Coal and bio-based materials are the major precursors for AC production, but coal is a fossil fuel with very high cost and non-sustainable, hence the latter is an indispensable alternative [15]. Nevertheless, abundant portion of waste bio-based materials in the world also serves as an environmental challenge. Similarly, the agricultural sector in Malaysia has been growing rapidly in the last decades, constituting over 2 million tons of agricultural waste generated annually and causing environmental menace [16]. Amongst these agricultural wastes is coconut shell, with about 63% production for domestic consumption in form of fresh coconut, tender coconut, coconut oil, and processed cream powders [16]. However, these wastes can be converted to value-added products like AC, hence solving disposal challenges.

The conventional method of activation results in surface heating from the furnace wall, which does not ensure a uniform temperature for different shapes and sizes of samples and generates a temperature gradient and high energy consumption. In recent years, microwave (MW) has emerged as a promising alternative energy source for the heating of materials, due to its numerous advantages like volumetric internal heating, uniform temperature distribution, rapid temperature rise, and energy saving [17–19]. Moreso, AC is known to be a good microwave absorber, and the regeneration and modification of ACs have been successfully conducted under microwave radiation [19,20]. In view of the advantages highlighted above, MW technique was employed for the activation process in this study.

However, the need for a more efficient and cost-effective AC production process led to the optimization of the production conditions using response surface methodology (RSM) [21–24]. RSM is a statistical technique for designing experiment, building models, evaluating the effects of several factors, and searching optimum conditions for desirable responses or using the experimental data obtained from specified experimental design to model and optimize any process in which a response (dependent variable) of interest is influenced by several independent variables (factors). It also helps in understanding the interactions among the parameters that have been optimized through analysis of variance (ANOVA), numeric and graphical analysis, respectively [21,25,26]. Another important advantage of RSM is the reduction in the number of experiments to be conducted as a result of simplified central composite design (CCD) factorial equation [18,27].

In order to obtain a high surface area of AC, the AC was produced by two-step activation process as it could enhance the surface area of the adsorbent [28,29].

To the best of our knowledge, two-step activation process in the synthesis of ACs from coconut shell with microwave and potassium hydroxide (KOH) as chemical activating agent using RSM for benzene and toluene removal is yet to be reported.

This study was carried out to optimize the conditions paramount for the production of AC from coconut shell for adsorption of benzene and toluene. CCD was chosen to evaluate the interaction of operating

conditions such as activating agent to precursor ratio, microwave power, and irradiation time, so as to optimize the preparation of coconut shell porous carbon for high yield and high removal percentage of benzene and toluene. Equilibrium, kinetic, and isotherms studies were also carried out to establish the correlation between the experimental and calculated values from the model equations.

2. Materials and methods

2.1. Materials

KOH, benzene, and toluene were purchased from Merck Chemicals Company, Malaysia. Coconut shells were taken from Johor state, Malaysia. The shells were adequately cleaned in distilled water and dried at 105°C for 48 h. After that, they were crushed and separated using sieves and shakers to the size range of 0.5–1.18 mm.

2.2. AC preparation

Preparation of the coconut shells for the AC synthesis was described in our previous study [30,31]. The coconut shell porous carbon was prepared with KOH as activating agent at different impregnation ratios (IRs) (1–3), and thereafter activated at microwave power levels (200–600 W) and irradiation times (0–12 min) as determined by the design of experiment table (Table 1). Two-step activation procedure was adopted from our previous study [29]. In two-step activation, the precursor is first carbonized and the resulting char is then activated; this helps to produce carbon with high specific surface area. Initial pyrolysis of the precursor was carried out in a furnace, under a flow of nitrogen (150 cm^3/min) from ambient temperature to pyrolysis temperatures (600–700°C) at 10°C/min heating rate for 1 through 4 h. The resulting char was activated in a microwave with different KOH IRs (mass ratio; g/g), microwave powers, and irradiation times as shown in Table 1. The mixture was mixed properly and dried in the oven for 24 h at 105°C before loaded into the glass reactor of the microwave and activated by heat treatment under a CO_2 flow of 150 cm^3/min at the designated power levels and irradiation times. Then, the AC was cooled and removed from the MW. The resultant activated samples were washed with distilled water and 0.1 M hydrochloric acid until the pH of the rinse was close to six and then dried at 105°C for 24 h. The resulting ACs were stored in desiccator prior to be used.

Table 1
Experimental design matrix and results

Run	Factor 1 Power level (X_1), W	Factor 2 Irradiation time (X_2), min	Factor 3 Impregnation ratio (X_3)	Response 1 Ben ads. (Y_1), %	Response 2 Tol. ads. (Y_2), %	Response 3 Yield (Y_3), %
1	600	8.0	2.0	72.2	40.8	76.2
2	400	6.0	1.0	65.0	70.0	77.0
3	200	8.0	2.0	59.8	30.8	92.4
4	400	0.0	2.0	76.5	55.0	98.0
5	300	4.0	2.5	70.0	70.0	89.6
6	500	4.0	1.5	84.0	85.0	95.0
7	500	12.0	2.5	83.4	66.8	86.2
8	400	8.0	3.0	80.6	50.0	87.0
9	500	4.0	2.5	82.0	36.0	93.0
10	300	12.0	1.5	82.6	60.4	70.0
11	500	12.0	1.5	82.2	65.2	74.1
12	400	8.0	2.0	78.0	76.0	87.0
13	300	4.0	1.5	83.0	63.6	93.0
14	400	6.0	0.0	36.5	32.2	70.0
15	400	8.0	2.0	76.0	70.0	85.0
16	400	6.0	2.0	80.0	79.0	89.0
17	300	12.0	2.5	60.4	36.4	93.6
18	400	8.0	2.0	82.4	70.0	89.5
19	400	8.0	2.0	79.4	75.0	85.0
20	400	16.0	2.0	79.8	52.0	67.6

2.3. Design of experiments

In the design of experiments, there are the dependent and independent variables which are referred to as factors and responses, respectively. In this study, the factors considered in the production of the adsorbent were based on the CCD, a feature of the RSM. The CCD method helps to reduce the number of experiments and in turn optimizes the factors by randomizing the experimental design and helps in fitting the quadratic surface, the synergistic interaction between the factors are also analyzed by the CCD [26]. The RSM consists of inbuilt mathematical and statistical models useful for the analysis of the combined effects of the factors on the responses of interest [27,31]. Other features of the CCD include 2^n factorial runs with $2n$ axial runs and n_c center runs. Based on preliminary studies and literature review, three factors were identified to be important variables influencing the characteristics of the produced AC. These factors were considered in this study and they include; (i) X_1, power level; (ii) X_2, irradiation time, and (iii) X_3, KOH IR. The ranges of these three factors were equally chosen based on literature and preliminary studies [26,31]. In the experimental design stage of the CCD as shown in Eq. 1, the three factors and their respective ranges resulted in eight factorial points, six axial points, and six replicates, showing a total of 20 random experiments to be conducted, and are presented in Table 1.

$$N = 2^n + 2n + n_c = 20 \tag{1}$$

where N is the total number of experiments required and n is the number of factors (3).

The validity and consistency of the experimental results were determined by the center points. The factors considered in this study were coded as high and low at −1 and +1 intervals, respectively. The randomization of the experimental sequence helps to reduce the influence of the unrestrained factors. The responses considered in this study are percentage removal of benzene (Y_1), percentage removal of toluene (Y_2), and AC yield (Y_3).

2.3.1. Model fitting and statistical analysis

Design Expert software version 7.1.6. (STAT-EASE Inc., Minneapolis, USA) was employed to carry out the regression analysis of the experimental results to establish its suitability with the generated equations and also to statistically determine the significance of the equations.

2.4. Batch equilibrium studies

Batch adsorption studies were done by agitating 0.1 g of the ACs with varying initial concentrations (50–250 mg/L) of VOC solution in Teflon covered 30 mL sample bottles at 30˚C in a shaker at 115 rpm. The VOC concentration was determined using UV–Vis spectrometer (Perkin Elmer Lambda 25) at 254 and 206 nm [9] for benzene and toluene, respectively. VOC uptake at equilibrium, Q_e (mg/g), was determined by:

$$Q_e = \frac{(C_o - C_e)V}{W} \tag{2}$$

where C_o and C_e (mg/L) are the concentrations of benzene and toluene at initial stage and at equilibrium. V (L) is the volume of solution, and W (g) is the mass of adsorbent.

2.4.1. Removal efficiency

The removal efficiency and adsorption capacity of benzene and toluene on the synthesized activated carbon (PHAC) were studied. The removal efficiency was calculated from the equation:

$$\% \text{ Removal} = \frac{C_o - C_e}{C_o} \times 100 \tag{3}$$

where C_o is the initial concentration of the VOCs and C_e is the final concentration of benzene and toluene at equilibrium.

2.5. Kinetics and equilibrium studies

Kinetics and equilibrium adsorption studies were done by agitating 0.1 g of the AC with varying initial concentrations (50–250 mg/L) of VOC solution in Teflon covered 30 mL sample bottles at 30˚C in a shaker at 115 rpm. The VOC concentration was determined at preset intervals using UV–Vis spectrometer (Perkin Elmer Lambda 25) at 254 and 206 nm for benzene and toluene, respectively, to reach equilibrium. VOC uptake at equilibrium, Q_e (mg/g), was determined by Eq. (3):

$$Q_t = \frac{(C_o - C_t)V}{W} \tag{4}$$

where C_o and C_t (mg/L) are the initial concentration and concentration at a particular time t, of benzene

and toluene; V (L) is the volume of the solution; and W (g) is the mass of the ACs.

2.6. AC yield

The carbon yield was calculated based on the following equation:

$$\text{Yield } (\%) = \frac{W_f}{W_i} \times 100 \quad (5)$$

where W_f and W_i are the final mass of AC (g) and the mass of char after carbonization (g), respectively.

2.7. Characterization of the prepared AC

Pore structural analysis was characterized with Micromeritics ASAP 2020 for full isotherm analysis. Scanning electron microscopy (SEM) analysis with Karl Zeiss (EVO50 XVPSEM, Germany) was carried out on PHAC to study the development of porosity and surface morphology. The surface organic structures of the AC was chemically and structurally studied by Fourier transform infra red spectroscopy (FT-IR) spectra recorded at 4 cm^{-1} of resolution and 16 scans min^{-1} between 4,000 and 370 cm^{-1} using a Perkin Elmer Spectrum one series model instrumental Analysis with the KBr disc method. The pH value of the precursor material (CS), coconut shell char (Char), and potassium hydroxide microwave activated carbon (PHAC) were estimated using the Japanese Industrial Standard, JIS Z 8802 [32]. Three grams of AC were soaked in a 100 mL of deionized water, boiled for 5 min, and the pH was immediately measured using a HANNA portable pH meter once the solution cooled to room temperature.

3. Results and discussion

3.1. Development of regression model equation

The correlation between the AC preparation factors and the percentage removal efficiency were established by the CCD of the RSM. Table 1 presents the experimental design matrix with the corresponding values of the responses obtained from the experimental studies. The percentage removal for benzene and toluene was in the ranges of 36.5–84% and 32.2–85%, respectively, while the yield of AC from the char was between 67.6 and 98%. From the model sum of squares, the highest order polynomial with significant values was selected.

After excluding the insignificant terms of the model, the final empirical equations for benzene removal efficiency (Y_1), toluene removal efficiency (Y_2), and yield (Y_3) are given in Eqs. (6)–(8), respectively:

$$Y_1 = 81.43 + 3.77x_1 + 0.27x_3 + 4.30x_1x_3 - 3.16x_1^1 - 2.60x_3^2 \quad (6)$$

$$Y_2 = 74.94 + 4.96x_1 + 0.50x_2 - 8.86x_3 + 5.94x_2x_3 - 9.89x_1^2 - 5.51x_2^2 - 3.30x_3^2 \quad (7)$$

$$Y_3 = 84.45 - 2.24x_1 \;\; 9.16x_2 + 0.34x_3 \quad (8)$$

The appearance of positive sign before the terms indicates synergistic effect, while negative sign is synonymous to antagonistic effect. The mean squares in the ANOVA for the surface response quadratic models were obtained by dividing the sum of the squares of each of variation sources, the model, and the error variance by the respective degrees of freedom. The correlation coefficients R^2 supporting the coordination between the optimization variables and the responses are 0.82 for benzene and 0.85 for toluene. This indicates that 82 and 85% of the total variation in the removal efficiency of benzene and toluene was ascribed to the experimental factors studied. The three variables, i.e. IR, power level, and irradiation time all contributed either individually or by way of interaction to the removal of both benzene and toluene as shown by the three-dimensional (3D) optimization in Figs. 1 and 2. Power level and IR significantly contributed to the adsorption process. This is shown in the quantum of their F-values of 4.92 and 6.48 for power level, respectively, as shown in Table 2. The contribution was attributed to the high MW power level needed for pores development and good impregnation for intercalation of potassium metal to the carbon material during activation [31].

3.2. Benzene and toluene (VOC) uptake

From the ANOVA analysis (Table 2) and Figs. 1 and 2, individual and synergistic effect of power level and chemical IR had more significant influence on the removal efficiencies of benzene and toluene, while irradiation time had the least influence on the removal

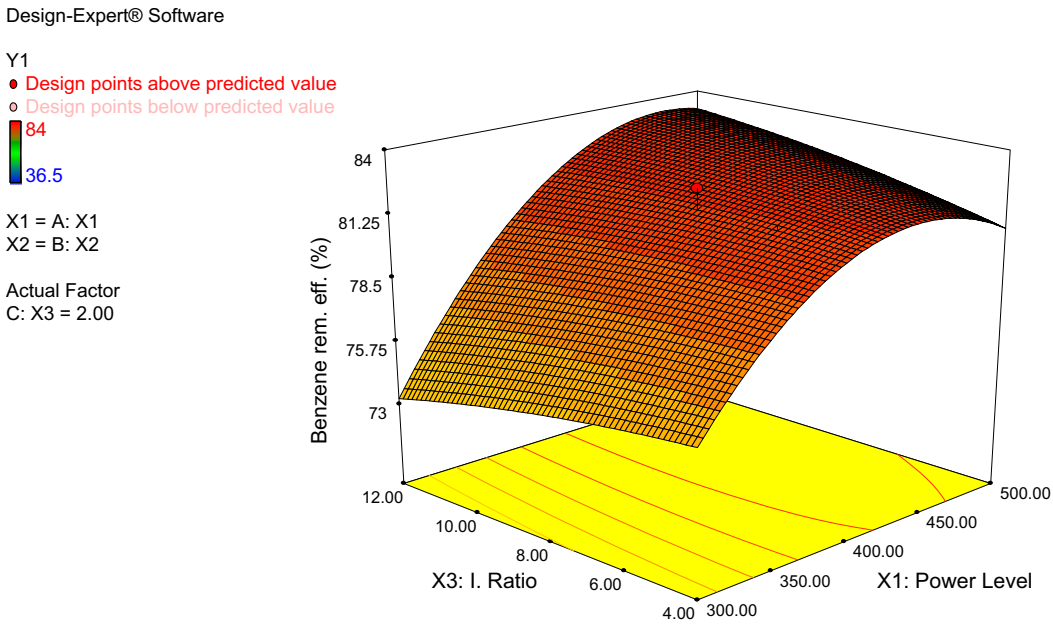

Fig. 1. A 3D response surface plot for benzene removal.

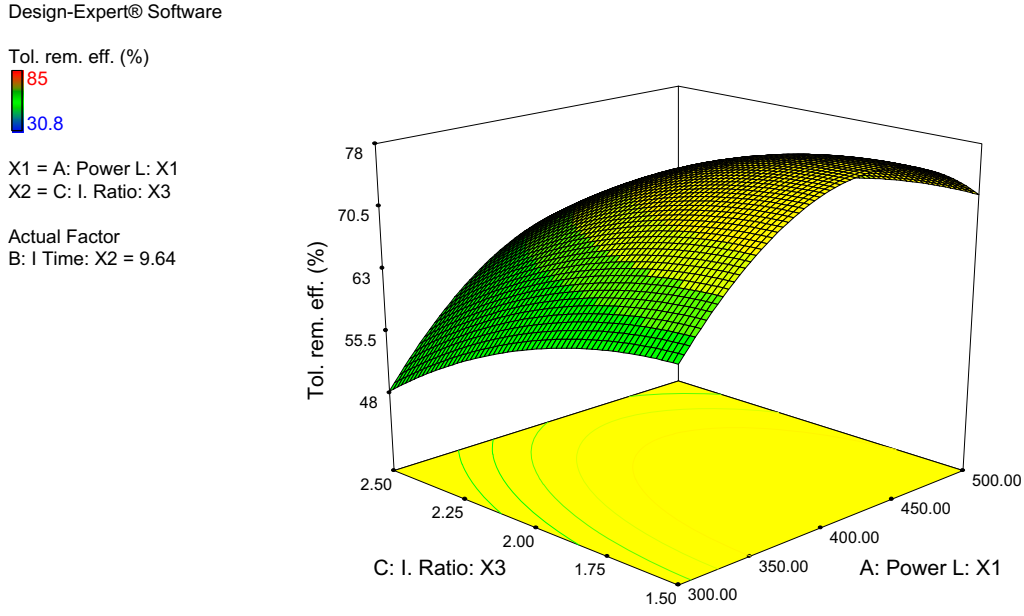

Fig. 2. A 3D response surface plot for toluene removal.

efficiencies of benzene and toluene by the produced AC. As for the benzene percentage removal (Y_1), the ANOVA result (Table 2) shows that the F-value of 5.12 and Prob > F values of 0.0088 were obtained from the selected model, which implies that the model is significant. Values of Prob > F less than 0.0500 indicate that the model terms are significant. In this case, X_1^2 and X_3^2 are significant model terms with Prob > F values of 0.0405 and 0.0037, respectively. This shows that the power level (X_1) and IR (X_3) have a greater influence on the AC production. The Lack of Fit F-values of 8.71 and 6.38 were obtained for benzene and toluene removal, these values are insignificant, and invariably means the model is suitable as the lack of it

Table 2
ANOVA for response surface quadratic model for benzene and toluene removal

	Benzene					Toluene				
Source	Sum of squares	df	Mean square	F value	p-value Prob > F	Sum of squares	df	Mean square	F value	p-value Prob > F
Model	2,134.16	9	237.13	5.12	0.0088	4,707.06	9	523.01	6.48	0.0036
X_1	228.01	1	228.01	4.92	0.0508	394.02	1	394.02	4.88	0.0516
X_2	0.02	1	0.02	5.3×10^{-4}	0.9821	4.04	1	4.04	0.050	0.8273
X_3	2.73×10^{-3}	1	2.73×10^{-3}	5.9×10^{-5}	0.9940	1,331.43	1	1,331.43	16.51	0.0023
X_1X_2	11.52	1	11.52	0.25	0.6288	15.13	1	15.13	0.19	0.6742
X_1X_3	147.92	1	147.92	3.19	0.1042	6.13	1	6.13	0.076	0.7885
X_2X_3	31.11	1	31.11	0.67	0.4315	293.95	1	293.95	3.64	0.0854
X_1^2	256.36	1	256.36	5.54	0.0405	2,364.13	1	2,364.13	29.31	0.0003
X_2^2	1.96	1	1.96	0.042	0.8412	717.12	1	717.12	8.89	0.0138
X_3^2	654.76	1	654.76	14.14	0.0037	1,202.87	1	1,202.87	14.91	0.0032

is expected to be insignificant for a good fit. While for toluene percentage removal (Y_2), the ANOVA result (Table 2) shows that the F-value of 6.48 and Prob > F values of 0.0036 were obtained from the selected model, which implies that the model is significant. In this case, X_3, X_1^2 and X_3^2 are significant model terms with Prob > F values of 0.0023, 0.0003, and 0.0032, respectively. This shows that the power level (X_1) and IR (X_3) have greater influence on the AC production. Micropollutants generally have molecular spherical diameters of about 0.55–1 nm [33]. This means that when more micropores are developed, more benzene and toluene molecules could be adsorbed by the ACs, therefore enhancing the adsorption capacity of the ACs. In this study, approximately 88% of the AC produced is in the microporous region which makes it more suitable for the adsorption of benzene and toluene.

3.3. Process optimization

Commercial production of ACs requires enormous yield and high removal efficiency of the adsorbent in order to be economically viable. The two aforementioned properties are necessary for the optimum performance and effectiveness of the AC for removal of benzene and toluene [26,31]. Optimization of these two essential responses concurrently is a bit challenging as the influence of the factors on the responses has different region of interest. The increase in one of the responses, say Y_1 or Y_2 leads to a decrease in Y_3 and vice versa. Hence, in order to reconcile these responses, another feature of the Design Expert software version 7.1.6 (STAT-EASE Inc., Minneapolis, USA) called desirability function was employed. These aforementioned responses were optimized under the same conditions. After which confirmatory experiments were conducted to validate the predicted responses obtained from the software. The experimental preparation conditions employed, predicted responses and experimental results for percentage benzene and toluene removal, and yield are presented in Table 3. The optimum conditions that gave rise to the optimized AC are 500 W power level, 4 min irradiation time, and 1.5 KOH IR which yielded 95% AC, 84% benzene removal efficiency, and 85% toluene removal efficiency, respectively. Similar trend was reported [26] for the adsorption of 2,4,6-trichlorophenol. The optimization of coconut shell AC carried out under microwave technique gave a good AC yield and VOCs removal efficiency which in turn could alleviate cost and save time.

3.4. Characterization of AC prepared under optimum condition (PHAC)

The SEM images of raw precursor (CS) and potassium hydroxide activated carbons (PHAC) are presented in Fig. 3(a) and (b). The surface morphology varies significantly with CS showing no pore formation due to the presence of volatiles and other contaminants on the surface, while the image of PHAC shows the formation of rudimentary pores as a result of volatilization of hemicellulose, cellulose, and lignin content of the raw coconut shell after carbonization, also, formation of some cavities and well-developed

Table 3
Model validation

			Percentage VOC removal (%)				Yield	
			Predicted		Experimental			
X_1 (W)	X_2 (min)	X_3, IR	Benzene	Toluene	Benzene	Toluene	Predicted	Experimental
500	4	1.5	83.17	75.5	84	85	91.03	95

pores were observed as a result of the space created by the evaporation of impregnated KOH derived compounds, and volatilization of the moisture and other impurities [31]. The pore widening and more developed pore structure observed in PHAC are also evident in the large BET surface area obtained. The BET surface area of was found to be 1,354 m^2/g and this can be compared with some ACs reported in the literatures having surface areas of 1,157 m^2/g [34], 167 m^2/g [14] and 183 m^2/g [35]. This pore widening mechanism is a result of the reaction between the chemical and the wall of the pores during the chemical activation process. Hence, higher pore widening was observed in PHAC.

3.5. Fourier transform infrared spectroscopy

FTIR spectrum analysis allows the identification of different functional groups on the surface of the adsorbent (PHAC). In Fig. 4, the spectrum shows the presence of some typical bands of lignocellulosic materials of coconut shell belonging to functional groups such as aromatic primary groups NH_2, hydroxyl, alkenes, aromatics, and carbonyls. The wideband at 3,500–3,100 cm^{-1} is ascribable to aromatic primary groups NH_2 and (O–H) vibrations in the hydroxyl groups [36]. This peak suggests the presence of nitrogen and phenolic groups after chemical activation with KOH. The band at 2,900–2,600 cm^{-1} is an indication of aldehydes. The vibrations between 2,400 and 2,100 cm^{-1} are alkyne functional groups. The vibrations between 1,700 and 1,550 cm^{-1} could be assigned to alkenes conjugation (C=C), i.e. the characteristics of cellulose and hemicelluloses [37]. The band at 1,200 and 1,100 cm^{-1} could be a result of C–O stretching vibrations in tertiary, secondary, and primary alcohol [38,39]. The bands centered in 1,050 through 600 and 550 cm^{-1} can be attributed to alkenes and aromatics out-of-plane bend with acyclic C–O–C groups conjugated with carbon–carbon double bounds (C=C–O–C) in olefinic or aromatic structures. While the vibrations in the range 900–700 cm^{-1} can be attributed to C–H deformation due to out-of-plane vibrations and can be assigned to the aromatic structures. The FT-IR result shows that the AC produced (PHAC) is rich in basic surface functional group which in turn helps in the adsorption process of hydrophobic contaminants like benzene and toluene. This basic characteristic is evident from the surface charge analysis conducted, with microwave AC (PHAC) and coconut shell char (CSC) having pH 10 and 8.3, respectively. While that of the coconut shell precursor material (CS) is slightly below the basic region with pH of 5.8. The high basicity in the AC by microwave than the char may be as a result of the microwave activation process which inherently improves basicity in ACs [19].

3.6. Surface area and pore volume of AC

The most important property of AC is its adsorptive capacity, which in general is proportional to the surface area. The carbonization process leads to the development of rudimentary pores in the char structure, making it more easily accessible for adsorbate. From Table 3, the BET surface area and pore volume for PHAC are 1,354 m^2/g and 0.61 cm^3/g, the result is relatively good compared to the values reported by [35] and [38].

Fig. 5 shows micropore and mesopore distributions with incremental pore volume that was ascertained using the density functional theory (DFT). PHAC is predominantly microporous with nearly 88% micropores and good pore development in the microporous region which ranges between 0.5 and 1.5 nm with peak at 0.6 nm. Some pore development was also observed in the mesoporous region (2–5 nm) which is almost linear to the x-axis as shown in the figure. The porosity parameters obtained from the N_2 adsorption isotherm are summarized in Table 4.

3.7. Effect of initial VOC concentration

The VOC concentration at equilibrium is measured at the point where the amount of VOC adsorbed on PHAC is in a state of dynamic equilibrium with the amount of VOC desorbing, and it reveals the

Table 4
Textural properties and surface charge of porous carbon prepared under optimized conditions

Samples	BET surfce area (m^2/g)	Micropore area (m^2/g)	External surface area (m^2/g)	Pore volume (cm^3/g)	Average pore width (nm)	Yield (%)	Surface charge (pH)
PHAC	1,354	894	459	0.61	2.4	95	10

maximum adsorption capacity of the PHAC. The result shows that equilibrium position was achieved more rapidly at lower initial VOC concentrations than at higher initial concentrations of VOC. This could be due to the fact that at lower concentrations, there is less number of VOC molecules competing for the vacant sites on PHAC and so, they will be adsorbed rapidly. While at higher concentrations, there are more molecules of VOC competing for the fixed PHAC dosage vacant sites available [40]. The effect of initial concentration on adsorption of benzene and toluene is shown in Figs. 6 and 7.

The adsorbates undergo movement from the bulk phase to the adsorbent external surface through a boundary layer, diffusion into the pores of the adsorbent and finally onto interior pores of the adsorbent [40]. Figs. 6 and 7 show the increase in adsorption capacity at equilibrium (Q_e) for benzene and toluene from 10.1 to 55.4 mg/g and 14.91 to 58.1 mg/g, respectively, with an increase in the initial VOCs concentrations from 50 to 250 mg/L. Therefore, it can be said that the adsorption of benzene and toluene on PHAC increased as the initial VOC concentration increases.

3.8. Adsorption equilibrium isotherm

Adsorption isotherm is useful in describing the interaction of solutes and adsorbent and how to optimize the use of the adsorbents. Langmuir, Freundlich, and Temkin isotherm models were studied with their evaluated parameters presented in Table 5. The Langmuir isotherm assumes monolayer adsorption and is given as:

$$Q_e = \frac{Q_m b C_e}{1 + bCe} \tag{9}$$

C_e (mg/L) is the adsorbate equilibrium concentration, Q_e (mg/g) is the quantity of adsorbate adsorbed per unit mass of adsorbent, Q_m and b are Langmuir constants which translate to the adsorption capacity and the intensity of adsorption, respectively [10,30]. A plot of Q_e against C_e gave a fitted curve (Figs. 8 and 9). The correlation coefficient R^2 of 0.99 indicated that the adsorption data of benzene and toluene on the PHAC was well fitted to the Langmuir isotherm.

Freundlich isotherm, on the other hand, assumes heterogeneous surface. The non-linear form of the Freundlich model is defined by:

$$Q_e = K_F C_e^{\frac{1}{n}} \tag{10}$$

where Q_e (mg/g) is the VOC equilibrium adsorption, C_e (mg/L) is the adsorbate equilibrium concentration, K_F and n are Freundlich constants. The value of n relates to the favorability of adsorption process and K_F

Table 5
Langmuir, Freundlich, and Temkin isotherm models constants, correlation coefficients of benzene and toluene adsorption on PHAC

Isotherms			Constants			
			Q_m (mg/g)	K_L (l/mg)	R^2	RSMD
Langmuir	PHAC	Benzene	212.77	0.0014	0.9978	1.76
		Toluene	238.10	0.0013	0.9976	2.15
			K_F (mg/g)	$1/n$	R^2	RSMD
Freundlich	PHAC	Benzene	0.49	0.8661	0.9942	1.95
		Toluene	0.48	0.8766	0.9927	2.33
			A (l/g)	b	R^2	RSMD
Temkin	PHAC	Benzene	0.0309	9.45	0.9603	3.05
		Toluene	0.0306	8.92	0.9466	3.40

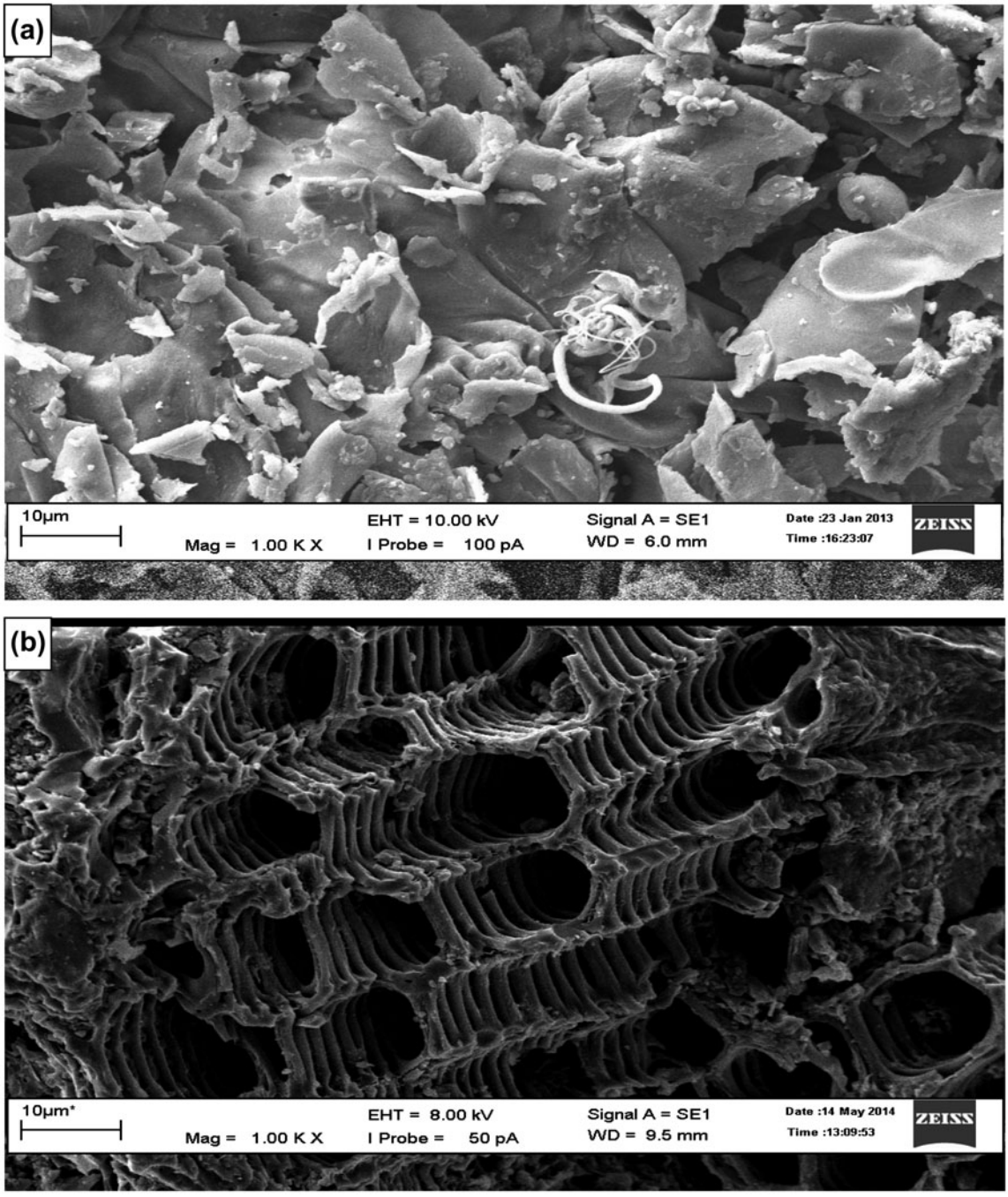

Fig. 3. SEM images of (a) raw coconut shell (CS) and (b) activated sample (PHAC).

represents the adsorption capacity. The slope of $1/n$ between 0 and 1 is a measure of the adsorption intensity or surface heterogeneity, becoming more heterogeneous as its value gets closer to zero [27,30]. The plot of Q_e vs. C_e (Figs. 8 and 9) gave a less fitted curve and lower R^2 value than Langmuir.

Lastly, the Temkin model equation is defined as:

$$Q_e = \frac{RT}{b} \ln AC_e \tag{11}$$

where A represents the maximum binding energy, b represents the heat of adsorption, Q_e (mg/g) is the

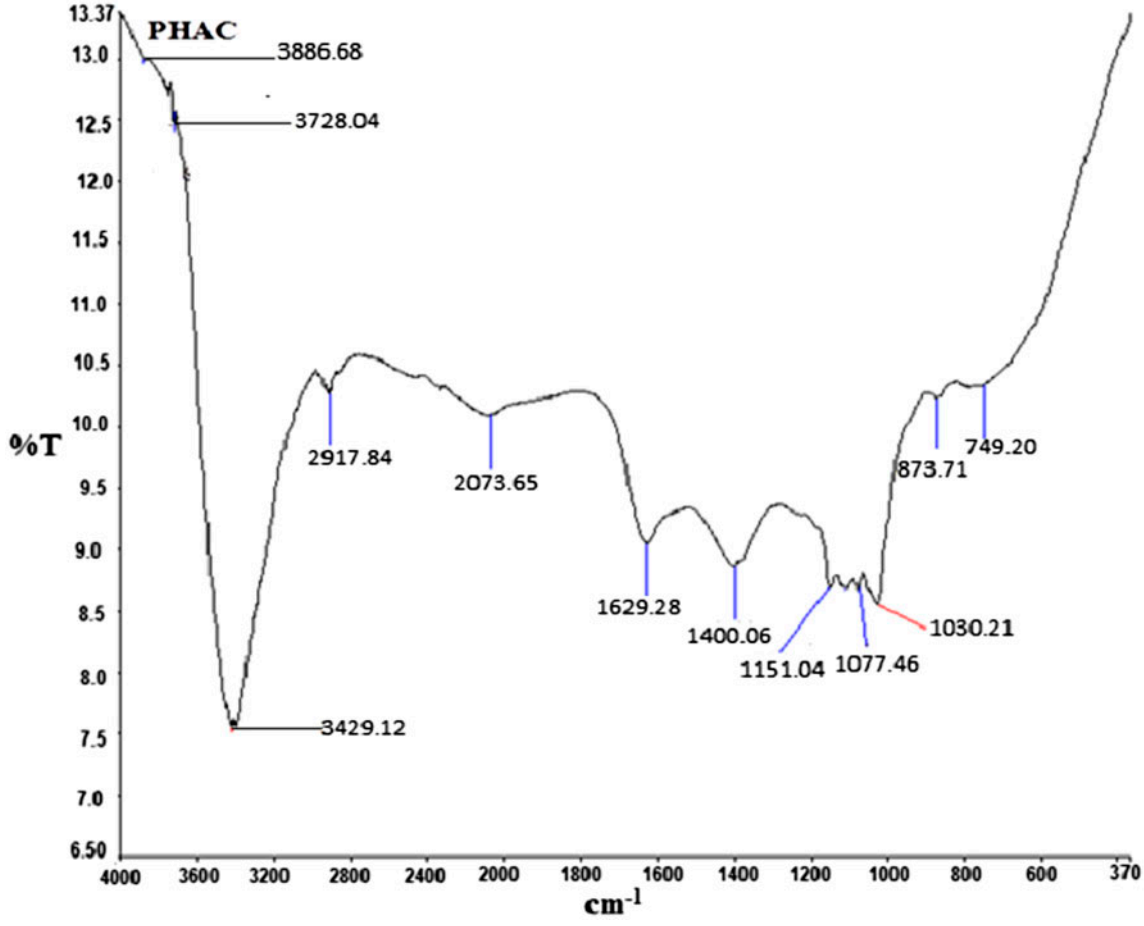

Fig. 4. The FT-IR for PHAC.

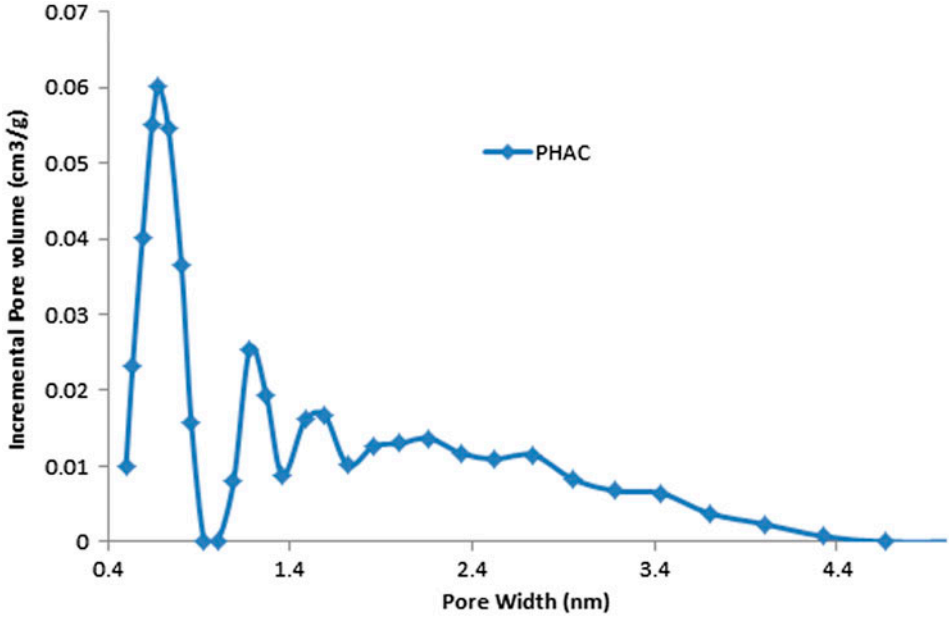

Fig. 5. DFT pore size distribution of activated carbon (PHAC).

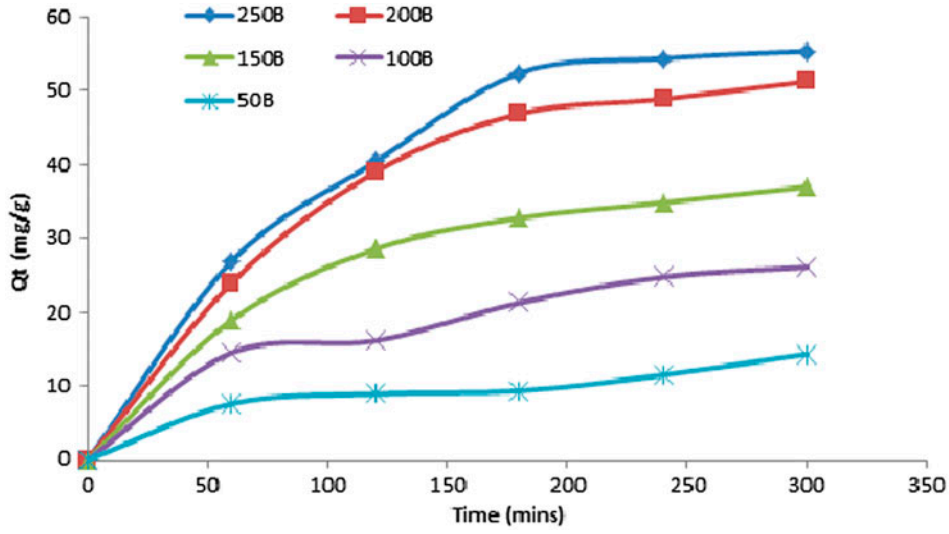

Fig. 6. Effect of initial concentration on adsorption of benzene on PHAC.

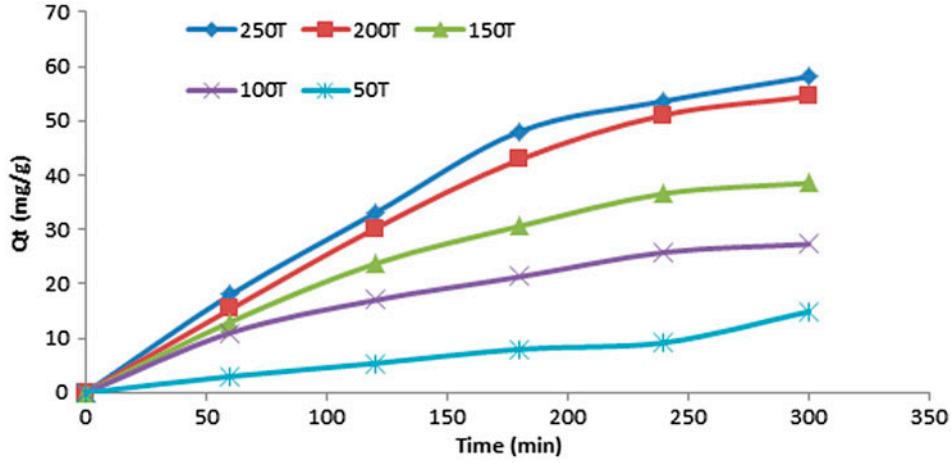

Fig. 7. Effect of initial concentration on adsorption of toluene on PHAC.

experimental adsorption capacity, and C_e (mg/L) is the VOC equilibrium concentration. A plot of Q_e against C_e gave good curves for both benzene and toluene (Figs. 8 and 9). However, Langmuir isotherm had the best fitting with maximum adsorption capacity of 212.77 and 238.10 mg/g on PHAC for benzene and toluene, respectively.

The models were further validated by root mean square deviation (RSMD) as enumerated in Table 5.

$$\text{RSMD} = \left[1/n \sum \left(q_{\text{exp}} - q_p\right)^2\right]^{1/2} \quad (12)$$

where n is the number of data points, q_{exp} (mg/g) and q_p (mg/g) are the experimental and calculated adsorption capacities, respectively. The lower the RMSD value the better the estimated model performs [12,30] with Langmuir model given the lowest RSMD values.

From Table 5, it is evident that PHAC had high benzene and toluene adsorption capacity (Q_m), this could be as a result of the well-developed surface morphology from the SEM result (Fig. 3(b)), also, the intensity of adsorption (b) shows that PHAC had good affinity for benzene and toluene and could be due to the higher surface area and pore volume recorded from the N_2 adsorption analysis.

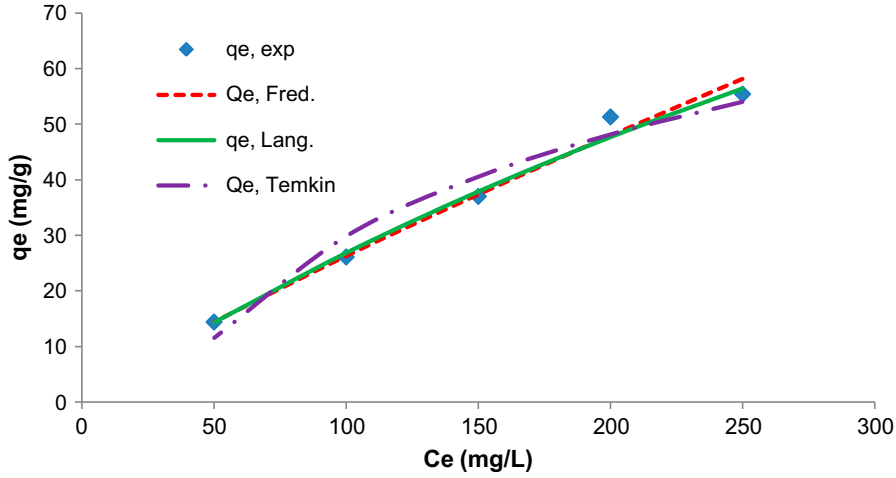

Fig. 8. Langmuir, Freundlich, and Temkin adsorption isotherms for benzene on PHAC.

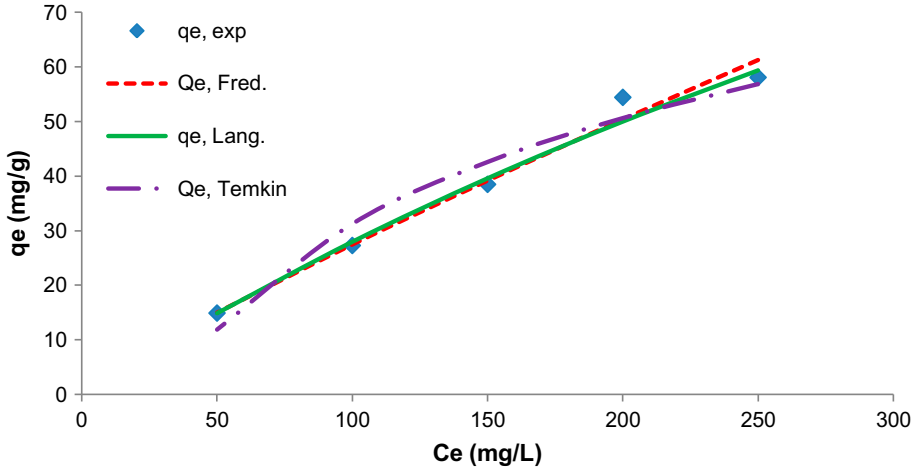

Fig. 9. Langmuir, Freundlich, and Temkin adsorption isotherms for toluene on PHAC.

The favorability of Langmuir isotherm can be expressed in terms of a dimensionless constant separation factor (R_L) defined by:

$$R_L = \frac{1}{1 + bC_o} \tag{13}$$

where b represents Langmuir constant and C_o (mg/L) represents highest VOC concentration. R_L value shows whether the isotherm is unfavorable ($R_L > 1$), linear ($R_L = 1$), favorable ($0 < R_L < 1$), or irreversible ($R_L = 0$). The values of R_L in this study were found to be 0.73 and 0.75 for adsorption of benzene and toluene, respectively, on PHAC. This indicates that Langmuir isotherm model was favorable.

The maximum adsorption capacity of benzene and toluene obtained in this work was compared with the literature (Table 6). It shows that the AC produced from this research performed better than the commercial AC (F-400), commercial AC chemically treated with nitric acid (F-400Cox) and the carbon nanotubes (CNTs) (Table 6), this could be as a result of the large surface area and pore volume obtained in PHAC. The commercial activated carbon (GAC) had adsorption capacity of 201.52 and 223.64 mg/g for benzene and toluene, respectively, slightly lower than the adsorption capacity obtained for PHAC with 212.77 and 238.10 mg/g for benzene and toluene, respectively. However, it is observed that the adsorption capacity of PHAC is slightly lower than the results reported by

Table 6
Comparison of maximum adsorption capacity (Q_m) of benzene and toluene on different porous carbons

Samples	Condition (°C)	Surface area (m^2/g)	Adsorption capacity (mg/g)		Ref.
			Benzene	Toluene	
Commercial activated carbon (F-400)	30	877.82	151.82	166.27	[9]
Commercial activated carbon chemically treated with nitric acid (F-400Cox)	30	938.36	90.82	98.34	[9]
Commercial activated carbon thermally treated (F-400Tox)	30	863.66	201.52	223.64	[9]
Carbon nanotubes (CNTs)	25	310.75	34.46	71.27	[8]
Oxidized carbon nanotubes CNT (NaOCl)	25	88.56	247.87	279.81	[8]
Commercial activated carbon (GAC)	25	1,292.10	217.32	221.13	[8]
PHAC	30	1,354	212.77	238.10	This work

[8] for oxidized carbon nanotubes (CNT(NaOCl)), with 247.87 and 279.81 mg/g obtained on CNT(NaOCl) for adsorption of benzene and toluene, respectively. This could be as a result of the modification of the CNT by NaOCl which may have enhanced its adsorption capacity for benzene and toluene.

3.9. Adsorption kinetics on VOC adsorption on AC

The kinetic models employed in this study are the pseudo-first-order, pseudo-second-order, and intraparticle diffusion equations which were used to determine the model that best described adsorption of benzene and toluene on PHAC. Pseudo-first-order model is given as:

$$\ln\,(q_e - q_t) = \ln q_e - k_1 t \tag{14}$$

where q_e and q_t are the quantity of benzene and toluene adsorbed (mg/g) at equilibrium and at time t (min), and k_1 is the adsorption rate constant (1/min). Values of k_1 were obtained from the slopes of the linear plots of $\ln(q_e - q_t)$ vs. t. The deviations of the calculated q_e values from the experimental q_e values were quite high (Table 7), signifying that this model was not appropriate.

Pseudo-second-order equilibrium adsorption is given by:

$$\frac{t}{q_t} = \frac{1}{k_2 q_e^2} + \frac{1}{q_e} t \tag{15}$$

where k_2 (g/mg min) is the second-order adsorption rate constant, q_e and k_2 can then be determined from the slope and the intercept of plot t/q_t vs. t. The linear plot demonstrates a good correlation between the experimental and the calculated q_e values (Table 7) indicating the applicability of the second-order model to describe the adsorption process.

On the other hand, intraparticle diffusion model was based on the theory proposed by Weber and Morris [14] to identify the diffusion mechanism. Intraparticle model is given by:

$$q_t = k_p t^{1/2} \tag{16}$$

where k_p is the intraparticle diffusion rate constant that is obtained from the slope of the straight line of q_t vs. $t^{1/2}$. The deviations between the experimental values obtained were the highest compared to those obtained from pseudo-first-order- and pseudo-second-order kinetic models indicating that it is not applicable in the adsorption process. However, the R^2 values of intraparticle diffusion are slightly higher than pseudo-first order and pseudo-second order for toluene adsorption most especially at lower concentrations. This may suggest that intraparticle diffusion is the rate-limiting step at lower concentrations of toluene adsorption onto PHAC.

Pseudo-second-order models had the best correlation in terms of the deviation between calculated and experimental values over the whole range of adsorption with chemisorption being the major rate-controlling step [41]. The results obtained in this study (Table 7) show that the deviation between the experimental results and calculated values for adsorption of benzene and toluene on PHAC were relatively lowest in the pseudo-second-order model, indicating that the values obtained from the pseudo-second-order model are more correlated to the experimental values, this is

Table 7
Parameters of pseudo-first-order, pseudo-second-order, and intraparticle diffusion models for benzene and toluene adsorption onto PHAC

VOC sample	Initial conc.	$q_{e,exp}$	Pseudo-first-order kinetic model			Pseudo-second-order kinetic model			Intraparticle diffusion model		
			$q_{e,cal}$	k_1	R^2	$q_{e,cal}$	k_2	R^2	$q_{e,cal}$	k_p	R^2
Benzene	250	55.4	65.41	0.013	0.9776	60.98	0.0231	0.9647	10.06	2.58	0.9409
	200	51.3	55.66	0.0133	0.996	56.82	0.0246	0.9651	28.72	2.38	0.8731
	150	37	36.67	0.012	0.9997	39.68	0.0295	0.9625	26.70	1.83	0.9456
	100	26.1	27.73	0.0112	0.9582	27.93	0.0241	0.9304	21.17	1.33	0.9561
	50	14.4	13.87	0.0076	0.9073	14.10	0.0234	0.8964	13.22	0.65	0.867
Toluene	250	58.1	85.63	0.0132	0.9464	71.42	0.0108	0.7692	−13.9	4.319	0.9757
	200	54.45	83.53	0.0134	0.9429	69.44	0.0092	0.708	16.58	4.2353	0.984
	150	38.5	52.14	0.0127	0.9609	46.08	0.0126	0.8219	22.92	2.7362	0.982
	100	27.3	33.19	0.0115	0.9624	30.96	0.0159	0.8822	21.24	1.7592	0.9912
	50	14.91	20.02	0.0076	0.7778	17.64	0.0056	0.4667	13.02	1.1338	0.9031

also evident in the higher values of the adsorption rate constant (k_2) when compared to the (k_1) values in pseudo-first-order model. The applicability of the pseudo-second-order model is more evident at higher initial concentrations of benzene as the correlation is more pronounced at (250 mg/L) with k_1 and k_2 values of 0.013 and 0.0231 obtained for benzene adsorption on PHAC. However, this is not the same with intraparticle diffusion of benzene and toluene on PHAC as the k_p values are higher than the k_2 values for all initial concentrations. This suggests that of chemisorption is most likely to be the rate-controlling steps for benzene and toluene adsorption on PHAC.

4. Conclusions

Microwave technique with the CCD of RSM was employed to optimize the preparation parameters for the production of high yield PHAC and subsequently applied for adsorption of benzene and toluene. The factors considered for the optimization are microwave power level, irradiation time, and IR. The optimum removal efficiencies for benzene and toluene are 84 and 85%, respectively, at 95% yield, the optimum condition at which these removal efficiencies were obtained are power level of 500 W, 4 min irradiation time, and 1.5 IR. Power level and chemical IR individually and synergistically had the best influence on the removal of benzene and toluene, respectively. Langmuir isotherm model best correlated the experimental data from the benzene and toluene removal efficiencies, while pseudo-second-order kinetic model best described the experimental results obtained for benzene and toluene removal by PHAC. From the textural characterization, BET surface area and pore volume of 1,354 m^2/g and 0.6 cm^3/g were obtained for PHAC while the average pore diameter was 1.8 nm. The SEM images show that PHAC had very well-developed pore structure and the FT-IR results show some basic functional groups on the AC. The optimization results show that the selected model was significant and correlated well with the experimental values, it also revealed that high removal efficiencies of benzene and toluene can be achieved from microwave irradiated AC which compares favorably well with commercial ACs from conventional techniques.

Acknowledgments

This study was supported by the University Research Grant (Q.J130000.2509.06H79) and International Doctoral Fund awarded by the Universiti Teknologi Malaysia, Johor Bahru.

References

[1] M.P. Abdullahi, S.S. Chian, Chlorinated and nonchlorinated-volatile organic compounds (VOCs) in drinking water of peninsular Malaysia, Sains Malys. 40 (2011) 1255–1261.
[2] L. Li, S. Liu, J. Liu, Surface modification of coconut shell based activated carbon for the improvement of hydrophobic VOC removal, J. Hazard. Mater. 192 (2011) 683–690.
[3] E.M. Abdullahi, M.A.A. Hassan, Z.Z. Noor, R.K.R. Ibrahim, Volatile organic compounds abatement from industrial wastewaters: Selecting the appropriate technology, Aust. J. Basic Appl. Sci. 12 (2013) 101–113.
[4] R.R. Bansode, J.N. Losso, W.E. Marshall, R.M. Rao, R.J. Portier, Adsorption of volatile organic compounds

by pecan shell and almond shell-based granular activated carbons, Bioresour. Technol. 90 (2003) 175–184.
[5] M.A. Lillo-Ródenas, A.J. Fletcher, K.M. Thomas, D. Cazorla-Amorós, A. Linares-Solano, Competitive adsorption of a benzene–toluene mixture on activated carbons at low concentration, Carbon 44 (2006) 1455–1463.
[6] J. Mohammed, N.S. Nasri, M.A.A. Zaini, U.D. Hamza, M.M. Ahmed, Optimization of preparation of microwave irradiated bio-based materials as porous carbons for VOCs removal using response surface methodology, Appl. Mech. Mater. 554 (2014) 175–179.
[7] M. Peng, L.M. Vane, S.X. Liu, Recent advances in VOCs removal from water by pervaporation, J. Hazard. Mater. 98 (2003) 69–90.
[8] F. Su, C. Lu, S. Hu, Adsorption of benzene, toluene, ethylbenzene and p-xylene by NaOCl-oxidized carbon nanotubes, Colloids Surf., A 353 (2010) 83–91.
[9] N. Wibowo, L. Setyadhi, D. Wibowo, J. Setiawan, S. Ismadji, Adsorption of benzene and toluene from aqueous solutions onto activated carbon and its acid and heat treated forms: Influence of surface chemistry on adsorption, J. Hazard. Mater. 146 (2007) 237–242.
[10] M.A.A. Zaini, R. Okayama, M. Machida, Adsorption of aqueous metal ions on cattle-manure-compost based activated carbons, J. Hazard. Mater. 170 (2009) 1119–1124.
[11] M.E. Abdullahi, M.A.A. Abu Hassan, Z.Z. Zainon Noor, R.K.R. Raja Ibrahim, Temperature and air–water ratio influence on the air stripping of benzene, toluene and xylene, Desalin. Water Treat. (2014) 1–8, doi: 10.1080/19443994.2014.903209.
[12] M. Auta, B.H. Hameed, Coalesced chitosan activated carbon composite for batch and fixed-bed adsorption of cationic and anionic dyes, Colloids Surf., B 105 (2013) 199–206.
[13] J. Mohammed, N.S. Nasri, M.A.A. Zaini, U.D. Hamza, M.M. Ahmed, Comparison on the characteristics of bio-based porous carbons by physical and novel chemical activation, Appl. Mech. Mater. 554 (2014) 175–179.
[14] N.S. Nasri, U.D. Hamza, S.N. Ismail, M.M. Ahmed, Assessment of porous carbons derived from sustainable palm solid waste for carbon dioxide capture, J. Cleaner Prod. 71 (2014) 148–157.
[15] K. Yang, J. Peng, C. Srinivasakannan, L. Zhang, H. Xia, X. Duan, Preparation of high surface area activated carbon from coconut shells using microwave heating, Bioresour. Technol. 101 (2010) 6163–6169.
[16] W.A.W.A.K. Ghani, M.S.F. Abdullah, K.A. Matori, A.B. Alias, G. Da Silva, Physical and thermochemical characterization of Malaysian biomass Ashes, J.—The Inst. Eng. Malys. 71 (2010) 9–18.
[17] Y.-B. Kim, J.-H. Ahn, Microwave-assisted decolorization and decomposition of methylene blue with persulfate, Int. Biodeterior. Biodegrad. 95 (2014) 208–211.
[18] D. Xin-hui, C. Srinivasakannan, P. Jin-hui, Z. Li-bo, Z. Zheng-yong, Comparison of activated carbon prepared from Jatropha hull by conventional heating and microwave heating, Biomass Bioenergy 35 (2011) 3920–3926.
[19] R. Hoseinzadeh Hesas, W.M.A. Wan Daud, J.N. Sahu, A. Arami-Niya, The effects of a microwave heating method on the production of activated carbon from agricultural waste: A review, J. Anal. Appl. Pyrolysis 100 (2013) 1–11.
[20] Q. Liu, T. Zheng, P. Wang, L. Guo, Preparation and characterization of activated carbon from bamboo by microwave-induced phosphoric acid activation, Ind. Crops Prod. 31 (2010) 233–238.
[21] A.A. Ahmad, B.H. Hameed, Effect of preparation conditions of activated carbon from bamboo waste for real textile wastewater, J. Hazard. Mater. 173 (2010) 487–493.
[22] M. Arulkumar, K. Thirumalai, P. Sathishkumar, T. Palvannan, Rapid removal of chromium from aqueous solution using novel prawn shell activated carbon, Chem. Eng. J. 185–186 (2012) 178–186.
[23] S. Chatterjee, A. Kumar, S. Basu, S. Dutta, Application of response surface methodology for methylene blue dye removal from aqueous solution using low cost adsorbent, Chem. Eng. J. 181–182 (2012) 289–299.
[24] M. Auta, J. Mohammed, B.L.T. Philip, A.A. Aboje, Preparation of activated carbon from oil palm fruit bunch for the adsorption of acid red 1 using optimized response surface methodology, J. Eng. Res. Apps. 2 (2012) 1805–1815.
[25] D.C. Montgomery, Design and Analysis of Experiments, fifth ed., Wiley, New York, NY, 2001.
[26] I.A.W. Tan, A.L. Ahmad, B.H. Hameed, Preparation of activated carbon from coconut husk: Optimization study on removal of 2,4,6-trichlorophenol using response surface methodology, J. Hazard. Mater. 153 (2008) 709–717.
[27] I.A.W. Tan, A.L. Ahmad, B.H. Hameed, Optimization of preparation conditions for activated carbons from coconut husk using response surface methodology, Chem. Eng. J. 137 (2008) 462–470.
[28] Y. Sun, P.A. Webley, Preparation of activated carbons from corncob with large specific surface area by a variety of chemical activators and their application in gas storage, Chem. Eng. J. 162 (2010) 883–892.
[29] N.S. Nasri, J. Mohammed, M.A.A. Zaini, R. Mohsin, U.D. Hamza, M.M. Ahmed, Synthesis and characterization of green porous carbons with large surface area by two step chemical activation with KOH, J. Tek. 67 (2014) 25–28.
[30] N.S. Nasri, J. Mohammed, M.A.A. Zaini, R. Mohsin, U.D. Hamza, M.M. Ahmed, Synthesis and characterization of bio-based porous carbons by two step physical activation with CO_2, J. Tek. 68 (2014) 5–9.
[31] M. Auta, B.H. Hameed, Optimized waste tea activated carbon for adsorption of Methylene Blue and Acid Blue 29 dyes using response surface methodology, Chem. Eng. J. 175 (2011) 233–243.
[32] JISC, Methods for Determination of pH of Aqueous Solutions (Japanese Industrial Standard, JIS Z 8802), Japanese Standards Association, Tokyo, 1984.
[33] J.K. Edzwald, Water Quality and Treatment: A Handbook of Drinking Water, American Water Works Association, Mc-Graw Hill, New York, NY, 2011, p. 14.13.
[34] E. Yagmur, M. Ozmak, Z. Aktas, A novel method for production of activated carbon from waste tea by chemical activation with microwave energy, Fuel 87 (2008) 3278–3285.
[35] W.M.A.W. Daud, W.S.W. Ali, Comparison on pore development of activated carbon produced from palm shell and coconut shell, Bioresour. Technol. 93 (2004) 63–69.

[36] K.Y. Foo, B.H. Hameed, Coconut husk derived activated carbon via microwave induced activation: Effects of activation agents, preparation parameters and adsorption performance, Chem. Eng. J. 184 (2012) 57–65.
[37] P. Chingombe, B. Saha, R.J. Wakeman, Surface modification and characterisation of a coal-based activated carbon, Carbon 43 (2005) 3132–3143.
[38] H. Demiral, I. Demiral, B. Karabacakoğlu, F. Tümsek, Production of activated carbon from olive bagasse by physical activation, Chem. Eng. Res. Des. 89 (2011) 206–213.
[39] J.M.V. Nabais, C.E.C. Laginhas, P.J.M. Carrott, M.M.L. Ribeiro Carrott, Production of activated carbons from almond shell, Fuel Process. Technol. 92 (2011) 234–240.
[40] I.A.W. Tan, A.L. Ahmad, B.H. Hameed, Adsorption of basic dye using activated carbon prepared from oil palm shell: Batch and fixed bed studies, Desalination 225 (2008) 13–28.
[41] K.Y. Foo, B.H. Hameed, Textural porosity, surface chemistry and adsorptive properties of durian shell derived activated carbon prepared by microwave assisted NaOH activation, Chem. Eng. J. 187 (2012) 53–62.